Journal of Southeast University (English Edition) Vol. 20 No. 3 Sept. 2004 ISSN 1003—7985

Dynamic characteristics of high speed angular-contact ceramic ball bearing

Xu Yanzhong Jiang Shuyun

(Department of Mechanical Engineering, Southeast University, Nanjing 210096, China)

Abstract: The dynamic characteristics of a high speed angular-contact ceramic ball bearing are studied and compared with that of the steel ball bearing. According to rolling bearing analysis theory, the bearing dynamic equations are established and are solved based on Hook-Jeeves's optimization theory on the computer. The results show that the bearing dynamic characteristics mainly depend on the rotational speed and ball material property at high speed. The bearing stiffness, notablely, initially decreases and then increases with increasing rotational speed. The ceramic ball bearing gains significant advantages over the steel ball bearing in high speed applications, such as lower contact stress, smaller deformation, less altering amount of contact angle, decreasing extent of variation of axial and radial stiffness and higher performance stability.

Key words: angular-contact bearing; ceramic ball; dynamic characteristics

As an emerging technology, high-speed machining leads to easier and more efficient material removal, improved surface finish, lower cutting force and decreased thermal effect. In the past few decades, the motorized-spindle was widely used in high-speed machining and the hybrid (steel/ceramic) angular-contact ball bearings are most popularly utilized to support the spindle shaft. The bearing dynamic characteristics are of vital importance to ensure desired product precision and directly influence the fatigue and wear life of the bearing. Conventionally, the bearing dynamic performance was always treated as a stable constant, even in high speed applications. Different from the low speed case, the dynamic characteristics of the bearing notablely depend on the rotating speed and ball material property at high speed. So there is an urgent requirement to study the nonlinear dynamic performance of the bearing, especially of the ceramic ball bearing at high speed.

Silicon nitride (Si_3N_4), has emerged as an extremely promising material for fabricating high performance all-ceramic or hybrid steel/ceramic rolling contact bearings. Compared with conventional steel bearings silicon nitride bearings have been shown to offer significant benefits in terms of rolling contact fatigue life, and the lower density of the material greatly reduces the dynamic loading at ball/raceway contacts at very high speed[1].

Received 2003-12-30.

Foundation items: The Natural Science Foundation of Jiangsu Province (No. BK2002059), the Key Technologies R&D Program of Jiangsu Province During the 10th Five-Year Plan Period (No.BE2003071).

Biographies: Xu Yanzhong (1970—), male, doctor, senior engineer; Jiang Shuyun (corresponding author), male, doctor, associate professor, Jiangshy@seu.edu.cn.

Various investigations have been done to study the dynamic characteristics of the angular ball bearings. The following facts have been acknowledged: ① The speed-dependent stiffness of the angular contact bearing decreases with the increasing rotational speed which consequently affects the spindle dynamics[2-4]. ② The initial axial preloading applied on the bearing plays a significant role to strengthen the bearing stiffness and reduce the vibration levels of the machine spindle[5,6]. But most papers have dwelled, to a considerable extent, upon bearing-shaft assembly; few researchers have made a complete and explicit analysis on bearing dynamic characteristics with the rotational speed ranging in large scale, especially for hybrid steel/ceramic angular-contact bearing. This paper studies the dynamic characteristics of the angular-contact bearing comprehensively under rotational speeds ranging from 0 to 10^5 r/min, so as to present the theoretical analytical data for hybrid angular-contact bearing application and lead to a better understanding of the bearing performance at high speed.

1 Bearing Dynamic Model

A typical angular-contact ball bearing in static state is shown in Fig. 1. The initial contact angles at outer and inner raceways are both α.

Fig. 2 illustrates the relative geometrical relationships between the ball and the raceways assuming that the outer raceway is fixed according to outer raceway control theory. Without rotation and preload, the outer raceway curvature center A and the inner raceway curvature center B are aligned with the ball center o, shown as the line AoB in Fig. 2, which indicates that

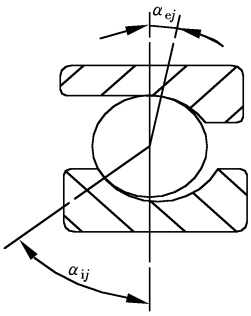

Fig.1 Angular-contact ball bearing without rotation and preload

the outer contact angle and the inner contact angle are the same. With the increasing rotating speed, centrifugal force and the gyroscopic moment will develop, which causes the ball center to migrate from o to o', and the inner raceway curvature center from B to B'. In turn, contact angles at the inner and outer raceways no longer remain the same and continually change with the rotational speed.

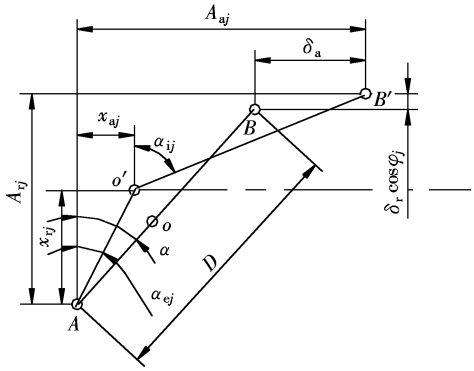

Fig.2 Positions of ball center and raceway groove curvature centers at high speed

The following equations were developed from Fig.2.

$$D = (f_e + f_i - 1) D_b \tag{1}$$

$$A_{aj} = D\sin\alpha + \delta_a \tag{2}$$

$$A_{rj} = D\cos\alpha + \delta_r \cos\psi_j \tag{3}$$

$$\cos\alpha_{ej} = \frac{x_{rj}}{(f_e - 0.5) D_b + \delta_{ej}} \tag{4}$$

$$\sin\alpha_{ej} = \frac{x_{aj}}{(f_e - 0.5) D_b + \delta_{ej}} \tag{5}$$

$$\cos\alpha_{ij} = \frac{A_{rj} - x_{rj}}{(f_i - 0.5) D_b + \delta_{ij}} \tag{6}$$

$$\sin\alpha_{ij} = \frac{A_{aj} - x_{aj}}{(f_i - 0.5) D_b + \delta_{ij}} \tag{7}$$

$$(A_{aj} - x_{aj})^2 + (A_{rj} - x_{rj})^2 - [(f_i - 0.5) D_b + \delta_{ij}]^2 = 0 \tag{8}$$

$$x_{aj}^2 + x_{rj}^2 - [(f_i - 0.5) D_b + \delta_{ej}]^2 = 0 \tag{9}$$

where D_b is the ball diameter, D_m is the bearing pitch diameter, δ_{ej} is the contact deformation between the j-th ball and the outer raceway, δ_{ij} is the contact deformation between the j-th ball and the inner raceway, f_i and f_e are the inner and outer raceway curvature coefficients, and ψ_j is the angular position of the j-th ball as shown in Fig.3.

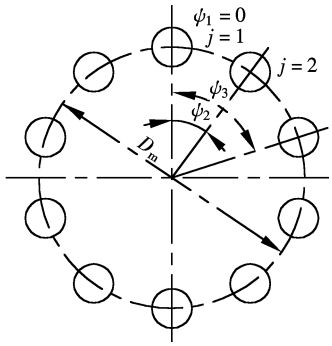

Fig.3 Angular position of the j-th ball

Fig.4 shows all the loads acting on the j-th ball, where F_{ej} is the frictional force, F_{cj} is the centrifugal force, M_{gj} is the gyroscopic moment, Q_{ej} is the outer contact force at the ball-raceway interface, Q_{ij} is the inner contact force at the ball-raceway interface.

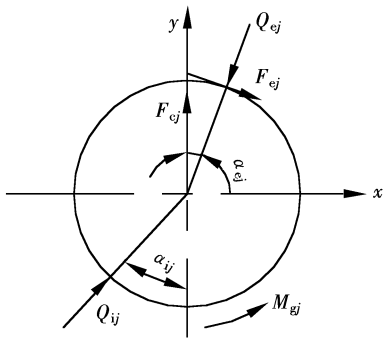

Fig.4 Load analysis of the j-th ball

The force equilibrium equations in the horizontal and vertical directions for the j-th ball can be obtained:

$$Q_{ij}\sin\alpha_{ij} - Q_{ej}\sin\alpha_{ej} + F_{ej}\cos\alpha_{ej} = 0 \tag{10}$$

$$Q_{ij}\cos\alpha_{ij} - Q_{ej}\cos\alpha_{ej} - F_{ej}\sin\alpha_{ej} + F_{cj} = 0 \tag{11}$$

Also, from the force equilibrium of the inner ring of the bearing, the following equations are established:

$$F_a - \sum_{j=1}^{z} Q_{ij}\sin\alpha_{ij} = 0 \tag{12}$$

$$F_r - \sum_{j=1}^{z} Q_{ij}\cos\alpha_{ij}\cos\psi_j = 0 \tag{13}$$

where F_a is the axial preload, and F_r is the radial force (constant). The contact forces Q_{ij} and Q_{ej} can be derived from Herz contact analysis and are represented by

$$Q_{ij} = K_{ij}\delta_{ij}^{\frac{3}{2}} \tag{14}$$

$$Q_{ej} = K_{ej}\delta_{ej}^{\frac{3}{2}} \tag{15}$$

where K_{ij} and K_{ej} are the functions of the curvatures of contact surfaces, the diameters of the bearing and

balls, and the types of material of the bearing ring and ball.

The gyroscopic moment M_{gj}, the frictional force F_{ej} and the centrifugal force F_{cj} are calculated respectively as follows:

$$M_{gj} = J\sin\beta\ \omega_{bj}\omega_{mj} \tag{16}$$

$$F_{ej} = \frac{2M_{gj}}{D_b} \tag{17}$$

$$F_{cj} = \frac{\pi}{12}\rho D_b D_m \omega_{mj}^2 \tag{18}$$

where ω_{mj} is the orbital speed of the j-th ball, ω_{bj} is the rotation speed of the j-th ball, and ρ is the density of the ball material. Based on the internal speeds and motions analysis of the bearing, ω_{mj} and ω_{bj} are expressed by

$$\omega_{bj} = \frac{\dfrac{\omega D_b \cos\beta_j}{D_m}}{\dfrac{\cos\alpha_{ej} + \tan\beta_j \sin\alpha_{ej}}{1 + \dfrac{D_b\cos\alpha_{ej}}{D_m}} + \dfrac{\cos\alpha_{ij} + \tan\beta\sin\alpha_{ij}}{1 - \dfrac{D_b\cos\alpha_{ij}}{D_m}}} \tag{19}$$

$$\omega_{mj} = \omega\frac{1 - \dfrac{D_b\cos\alpha_{ij}}{D_m}}{1 + \cos(\alpha_{ij} - \alpha_{ej})} \tag{20}$$

where ω is the rotational speed of the inner ring, β_j is the angle between the rotational plane and the plane normal to the axis of rotation of the j-th ball and is given by

$$\tan\beta_j = \frac{\sin\alpha_{ij}}{\cos\alpha_{ej} + \dfrac{D_b}{D_{mj}}} \tag{21}$$

So far, a group of nonlinear equations can be obtained including Eqs. (8) − (13). It should be noted that Eqs. (8) − (11) can be established for every ball, so the number of the total Eqs. (8)−(13) is $4z + 2$ in which z denotes the number of balls. Given F_a, F_r, ω, D_m, D_b and z as input conditions, the values δ_{ej}, δ_{ij}, x_{rj}, x_{aj}, δ_a and δ_r can be determined by solving the equation group. The axial stiffness K_a and the radial stiffness K_r can be given by

$$K_a = \frac{dF_a}{d\delta_a} \approx \frac{\Delta F_a}{\Delta\delta_a} \tag{22}$$

$$K_r = \frac{dF_r}{d\delta_r} \approx \frac{\Delta F_r}{\Delta\delta_r} \tag{23}$$

2 Bearing Dynamics Analysis

A computer program based on the Hook-Jeeves search technique[7] was developed to solve the group of nonlinear equations (8) − (13). With given shaft rotational speed, axial preload and radial load, the solving method requires the initial guesses for δ_{ej}, δ_{ij}, x_{rj}, x_{aj}, δ_a and δ_r, taking j, in turn, from 1 to z. Based on the initial guesses, the program searches for the minimum value of the square sum of equations given by Eqs. (8) − (13). When the value is minimized to meet the desired tolerance, the corresponding values of δ_{ej}, δ_{ij}, x_{rj}, x_{aj}, δ_a and δ_r are yielded. The bearing stiffness can then be obtained from Eqs. (22) and (23). Consequently other parameters, such as contact angle, gyroscopic moment, centrifugal force, contact stress, can also be calculated according to *Rolling Bearing Analysis*[8]. The specifications of angular-contact bearing used for analysis are listed in Tab.1.

Tab.1 Specifications of the bearing

Item	Specification
z	16
Initial contact angle α/(°)	15
D_b/mm	7.144
D_m/mm	43.5
Inner and outer groove radius/mm	3.72
Material type of ball	Steel/ceramic
Material type of bearing rings	Steel

2.1 Centrifugal force and gyroscopic moment

Fig. 5 and Fig. 6 show the increase of the centrifugal force and gyroscopic moment acting on a single ball with respect to the rotational speed under fixed preload F_a = 300 N. As shown in Fig. 5, the centrifugal force increases considerably with the

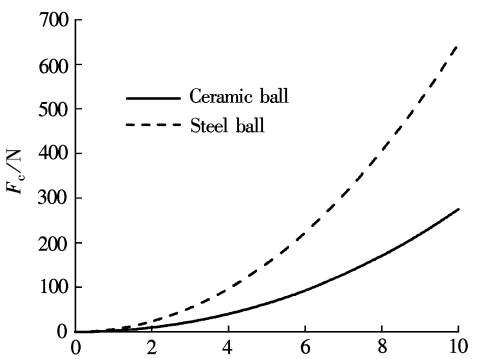

Fig.5 Centrifugal force vs. rotational speed (F_a = 300 N)

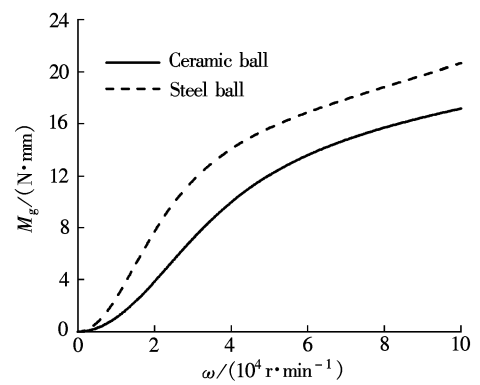

Fig.6 Gyroscopic moment vs. rotational speed (F_a = 300 N)

increasing rotational speed, and the steel ball centrifugal force is as about three times that of the ceramic ball. Large centrifugal force is the ultimate main factor influencing the dynamic performance at high speed. Gyroscopic moment M_g tends to cause the ball to slide along the raceway and is resisted by frictional force F_e(see Fig.4). The sliding motion will occur if the moment is excessively high, then cause undesirable wear and heat in bearing. It is apparent that the ceramic ball generates less centrifugal force and gyroscopic moment than the steel ball.

2.2 Contact angle

Once the bearing begins to rotate, centrifugal force will develop, which causes the outer contact angle to decrease and the inner contact angle, in contrast, to increase so as to balance the load induced by the rotating speed. Both the ball and the inner raceway curvature centers will move their positions (see Fig. 2). Fig. 7 shows the change of the contact angle with respect to rotational speed. Also, contact angle of steel ball bearing varies more violently than that of the ceramic ball bearing.

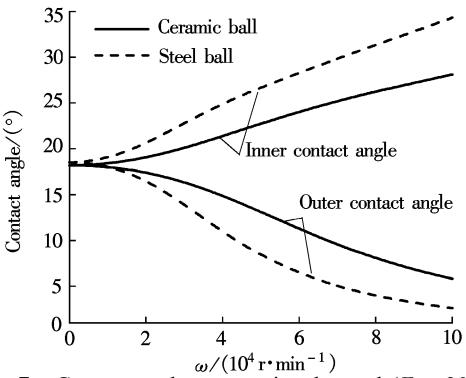

Fig.7 Contact angle vs. rotational speed (F_a = 300 N)

2.3 Contact stress and deformation

Fig. 8 and Fig. 9 demonstrate the contact stress and deformation variation with rotational speed ranging from 0 to 10^5 r/min under the axial preload F_a = 300 N.

Because the contact area is very small, the contact stress induced is usually very large, although the load is moderate. In Fig. 8, the maximum stress rises high to 2. 8 GPa in the steel ball bearing at the speed 10^5 r/min but it is lower in the ceramic ball due to its density being only about 1/3 that of the steel bearing, which will greatly reduce centrifugal force. As the centrifugal force acts entirely on the outer contact surface, the outer contact stress and deformation increase sharply with the increasing speed, whereas the inner contact stress and deformation decrease slightly.

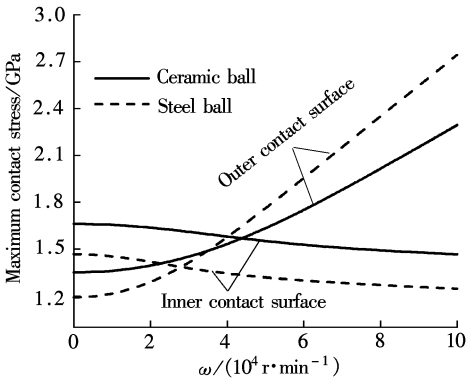

Fig.8 Maximum contact stress vs. rotational speed (F_a = 300 N)

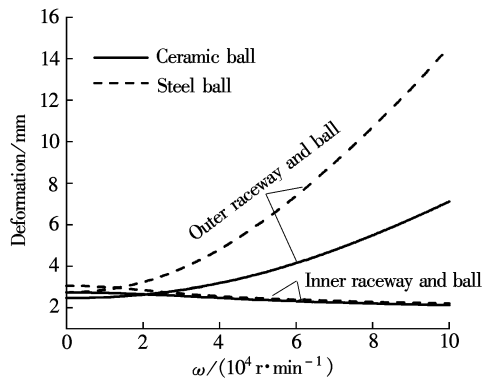

Fig.9 Deformation vs. rotational speed (F_a = 300 N)

It should be noted that large deformation leads to performance instability of the bearing, high stress reduces the bearing fatigue life and generates more heat derived from friction, so the ceramic ball bearing is more suitable for a high-speed spindle than the steel ball bearing.

2.4 Axial and radial stiffness

Stiffness plays the most important role in bearing dynamic performance and is the crucial factor influencing spindle dynamics. Fig.10 and Fig.11 show the significant variation of the axial and radial stiffness with the rotational speed under different axial preloads F_a. As illustrated in two figures, both axial and radial stiffness initially decrease and then ascend along with the increasing rotational speed. The stiffness is related to the contact area and contact angle on both raceways. A larger contact area tends to enhance the stiffness, but the smaller outer contact angle and the bigger inner contact angle tend to weaken the stiffness. The stiffness value depends on those factors above.

Apparently, higher preload results in higher bearing stiffness. But alternatively too much preload will generate an excessive amount of heat and shorten the bearing life. Both figures verify, again, the ceramic ball bearing's advantages over the steel ball bearing.

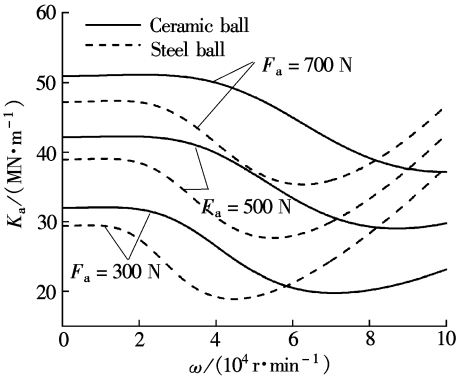

Fig.10 Bearing axial stiffness vs. shaft speed

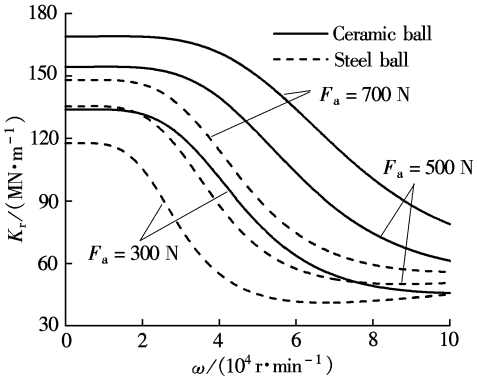

Fig.11 Bearing radial stiffness vs. shaft speed

3 Conclusions

1) The analytical models have been derived for the angular-contact ceramic ball bearings. The dynamic characteristics of the bearing are studied and compared with that of the steel ball bearing.

2) At high speed, the bearing dynamic characteristics depend to a greater extent on the rotational speed and ball material property besides preload. The bearing stiffness significantly decreases initially and then increases with increasing rotational speed, which differs from that at low speed.

3) The ceramic ball bearing is evidently more advantageous to be employed as the high-speed spindle bearing than the steel one.

References

[1] Wang L, Snidle R W, Gu L. Rolling contact silicon nitride bearing technology: a review of recent research[J]. *Wear*, **2000, 246**: 159－173.

[2] Lee Dong-Soo, Choi Dong-Hoon. Reduced weight design of a flexible rotor with ball bearing stiffness characteristics varying with rotational speed and load[J]. *Vibration and Acoustics*, *Transactions of the ASME*, **2000, 122**(3): 203－208.

[3] Jorgensen Bert R, Shin Yung C. Dynamics of spindle-bearing systems at high speeds including cutting load effects [J]. *Manufacturing Science and Engineering*, **1998, 120**(2): 387－394.

[4] Lynagh N, Rahnejat H, Ebrahimi M, et al. Bearing induced vibration in precision high speed routing spindles[J]. *International Journal of Machine Tools and Manufacture*, **2000, 40**: 561－577.

[5] Alfares Mohammed A, Elsharkawy Abdallah A. Effects of axial preloading of angular contact ball bearings on the dynamics of a grinding machine spindle system [J]. *Journal of Materials Processing Technology*, **2003, 136**(1): 48－59.

[6] Lin Chi-Wei, Tu Jay F, Kamman Joe. An integrated thermo-mechanical-dynamic model to characterize motorized machine tool spindles during very high speed rotation [J]. *International Journal of Machine Tools and Manufacture*, **2003, 43**(10): 1035－1050.

[7] Gottfried B S, Weismann J. *Introduction to optimization theory* [M]. New Jersey: Prentice-Hall, 1973. 113－130.

[8] Harris Tedric A. *Rolling bearing analysis*. 2nd Ed[M]. New York: John Wiley & Sons, Inc, 1984. 119－278.

高速角接触陶瓷球轴承动态特性研究

徐延忠　　蒋书运

(东南大学机械工程系, 南京 210096)

摘要: 根据滚动轴承的分析理论建立了轴承的动态数学模型并通过 Hook-Jeeves 的优化方法求解, 研究了高速角接触陶瓷球轴承的动态特性, 并与传统的钢轴承作了对比. 结果表明: 与低转速工况时相比, 高转速时轴承的动态性能不仅受预加载荷的影响, 而且在更大程度上与转速和滚珠材料特性有关; 随转速的升高, 轴承的轴向刚度与径向刚度均发生显著变化, 变化趋势为先下降后上升; 在高速状态下, 与传统钢轴承相比, 陶瓷球轴承的接触应力及变形明显降低、接触角变化较小、轴向与径向刚度变化程度相对较低、动态特性相对稳定, 从而具有传统钢球轴承无可比拟的优越性.

关键词: 角接触轴承; 陶瓷球; 动态特性

中图分类号: TH132